Journal of Coordination Chemistry

ISSN: 0095-8972 (Print) 1029-0389 (Online) Journal homepage: http://www.tandfonline.com/loi/gcoo20

Synthesis and DNA studies of a copper(II) complex of 5,6-dihydro-5,6-epoxy-1,10-phenanthroline

Sekar Baskaran, Mani Murali Krishnan & Mahadevimangalam Narayanasamy Arumugham

To cite this article: Sekar Baskaran, Mani Murali Krishnan & Mahadevimangalam Narayanasamy Arumugham (2015) Synthesis and DNA studies of a copper(II) complex of 5,6-dihydro-5,6-epoxy-1,10-phenanthroline, Journal of Coordination Chemistry, 68:24, 4395-4407, DOI: 10.1080/00958972.2015.1088526

To link to this article: http://dx.doi.org/10.1080/00958972.2015.1088526

Journal of Coordination Chemistry, 2015
Vol. 68, No. 24, 4395–4407, http://dx.doi.org/10.1080/00958972.2015.1088526

Synthesis and DNA studies of a copper(II) complex of 5,6-dihydro-5,6-epoxy-1,10-phenanthroline

SEKAR BASKARAN, MANI MURALI KRISHNAN and MAHADEVIMANGALAM NARAYANASAMY ARUMUGHAM*

Department of Chemistry, Thiruvalluvar University, Vellore, India

(*Received 1 September 2014; accepted 14 August 2015*)

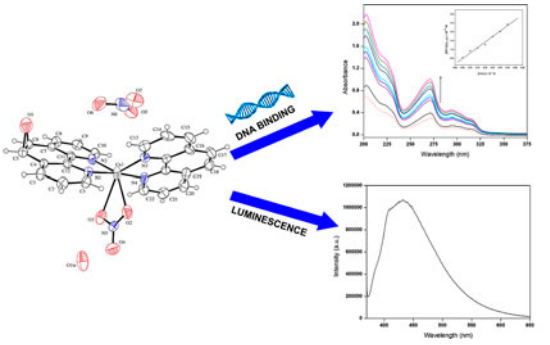

A new copper(II) complex, $[Cu(epoxy)(phen)(NO_3)](NO_3)\cdot H_2O$ (epoxy = 5,6-dihydro-5,6-epoxy-1,10-phenanthroline, phen = 1,10-phenanthroline), has been synthesized and characterized by elemental analysis, IR and UV–vis spectroscopy, and single crystal X-ray diffraction. The complex crystallized in a monoclinic system with space group *P21/n*, $a = 13.3199(8)$ Å, $b = 11.2917(7)$ Å, $c = 16.0832(9)$ Å, $\alpha = 90°$, $\beta = 107.827(4)°$, and $\gamma = 90°$. The complex cation possesses a distorted octahedral geometry, with Jahn–Teller distortion occurring in the CuN_4O_2 core. The binding interaction with calf thymus DNA (CT–DNA) was investigated by UV–vis and fluorescence spectroscopy, cyclic voltammetry, and viscometry. The results support a partially intercalative binding mode. Efficient cleavage of plasmid DNA by the complex was observed by gel electrophoresis.

Keywords: Six-coordinate copper(II); Epoxy-phenanthroline; Fluorescence; DNA binding; DNA cleavage

1. Introduction

Copper is an important micro-nutrient and plays a prominent role in proper functioning of organs and metabolic processes. It also acts as an essential cofactor for tumor angiogenesis-related processes [1]. Copper complexes are an attractive prospect as therapeutics, since

*Corresponding author. Email: aru_mugham@yahoo.com

copper is an essential element in biological systems, playing a vital role in biological processes, such as electron transfer, oxygen transport, and endogenous oxidative DNA damage associated with aging and cancer [2].

Copper(II) complexes of heterocyclic bases have become of particular interest subsequent to the discovery of the 'chemical nuclease' activity of $[Cu(phen)_2]^{2+}$ [3]. Furthermore, many copper(II) complexes have shown strong interactions with DNA via surface association or intercalation [4, 5]. 1,10-Phenanthroline (phen) is a planar and classic chelating ligand for transition metal ions, and is one of the most widely used ligands in modern coordination chemistry [6–9]. This heterocyclic sp^2 nitrogen donor ligand is more rigid than its well-known congener 2,2′-bipyridine (bpy). This rigidity is brought about by the central ring, resulting in the juxtaposition of the two nitrogen donors. This is advantageous in that it leads to rapid formation of complexes with metal ions. Applications of metal complexes incorporating 1,10-phenanthroline are numerous [10–12]. The 5,6-double bond in 1,10-phenanthroline is most susceptible to electrophilic attack, and even epoxide derivatives can be formed, such as 5,6-dihydro-5,6-epoxy-1,10-phenanthroline [13, 14]. Epoxides serve as useful starting materials in the synthesis of a variety of functionalized organic compounds, as the epoxide ring reacts readily with a wide range of nucleophiles with high regioselectivity [15, 16].

In continuation of our work in this area [17, 18], herein, we report the synthesis and structural characterization of a new octahedrally coordinated copper(II) complex $[Cu(epoxy)(phen)(NO_3)](NO_3)\cdot H_2O$ from 5,6-dihydro-5,6-epoxy-1,10-phenanthroline and 1,10-phenanthroline. The photoluminescence properties, DNA binding, and cleavage activity of the mixed-ligand epoxy copper(II) complex were also studied.

2. Experimental

2.1. *Materials and instrumentation*

General chemicals, such as methanol, anhydrous diethyl ether, $Cu(NO_3)_2\cdot 3H_2O$, and 1,10-phenanthroline monohydrate are all analytical grade and used as received. Plasmid pBR322 DNA was purchased from Bangalore Genie (India). 5,6-Dihydro-5,6-epoxy-1,10-phenanthroline, disodium salt of calf thymus DNA (CT–DNA), Tris(hydroxymethyl)aminomethane (Tris), and ethidium bromide (EtBr) were purchased from Sigma–Aldrich (USA).

The infrared spectra were recorded on a Perkin Elmer spectrometer as KBr pellets (4000–400 cm^{-1}), and elemental analysis was performed on a Perkin Elmer-240C micro analyzer. UV-vis and fluorescence spectra of the complex were recorded on a Shimadzu UV-2450 spectrophotometer and Jobin Young Fluorolog 3 spectrophotometer, respectively. Molar conductivity measurements were done using an Equip-Tronics (India) conductivity meter model number EQ-665. Cyclic voltammetry (CV) experiments were recorded on CHI 602D (CH Instruments Co., USA) electrochemical analyzer under oxygen-free conditions using a three-electrode cell in DMF solution with TBAP (0.1 M) as the supporting electrolyte. A platinum wire, glassy carbon (GC), and Ag/AgCl (in saturated KCl solution) electrodes were used as counter, working and reference electrode, respectively.

2.2. *Synthesis of [Cu(epoxy)(phen)(NO$_3$)](NO$_3$)·H$_2$O*

To a methanolic solution (10 mL) of 5,6-dihydro-5,6-epoxy-1,10-phenanthroline (392.4 mg, 2 mmol), $Cu(NO_3)_2\cdot 3H_2O$ (483.0 mg, 2 mmol) dissolved in methanol (10 mL) was added

dropwise with vigorous stirring. After 30 min, the methanolic solution (10 mL) of 1,10-phenanthroline monohydrate (396.4 mg, 2 mmol) was added slowly, and then the solution was stirred for about 6 h at ambient temperature. The resulting faint green solution was filtered and kept for slow evaporation. After a week, a suitable green crystal separated for XRD experiments. It was filtered and washed with cold methanol and diethyl ether. Yield: 60%. Analytical calculation for $C_{24}H_{16}CuN_6O_8$ (%): C, 49.70; H, 2.78; N, 14.49. Found (%): C, 49.62; H, 2.59; N, 14.55. IR (KBr, cm^{-1}): 3500br, 3054 m, 2426w, 1583s, 1518s, 1427 m, 1383vs, 1289w, 1031s, 853s, 722vs (br, broad; vs very strong; s, strong; m, medium; w, weak). UV–vis (H_2O), λ/nm ($\varepsilon/M^{-1}\,cm^{-1}$): 271 (12,720) and 295 (6340) (π–π^*); 315 (4150; n–π^*), 705 (67; d → d). Conductance Λ_M ($\Omega^{-1}\,cm^2\,mol^{-1}$) in water at 27 °C: 98. μ_{eff} = 1.79 BM at 298 K.

2.3. *X-ray crystallography*

An X-ray diffraction study was carried out using a Bruker Kappa Apex-II single crystal X-ray diffractometer equipped with MoKα (λ = 0.71073 Å) radiation. A green crystal ($0.25 \times 0.20 \times 0.20\ mm^3$) was cut and mounted on a glass fiber using cyanoacrylate. The unit cell parameters were determined from 36 frames measured from three different crystallographic zones and using the method of difference vectors. Indexing for cell parameters showed that the compound crystallized in the monoclinic system with *P21/n* space group. The collected intensity data frames were integrated, Lorentz–Polarization correction, and decay correction were done using SAINT-plus software [19]. Empirical absorption correction (multi-scan) was performed using SADABS [20]. The structure was solved by direct methods using SIR92 [21], followed by the refinement by full-matrix least squares refinement on F^2 using the SHELXTL-97 program [22]. All non-hydrogen atoms were refined anisotropically and all hydrogens could be located on the difference Fourier map. The CCDC deposition number of the crystal was 973086.

2.4. *Spectroscopic studies on DNA interaction*

2.4.1. Electronic absorption spectra. The DNA binding experiments were performed at room temperature. The DNA concentration per nucleotide was determined by electronic absorption spectroscopy using 1 cm path length cuvettes. DNA solutions in 5 mM Tris–HCl/50 mM NaCl buffer, pH 7.1 gave the ratio of UV absorbance at 260 and 280 nm, A_{260}/A_{280}, of 1.9, indicating that the DNA was sufficiently free of protein [23]. The DNA concentration was determined by measuring the UV absorption at 260 nm, taking the molar absorption coefficient (ε_{260}) of CT-DNA as $6600\ M^{-1}\,cm^{-1}$ [24]. Absorption titration experiments of copper(II) complex in Tris–HCl buffer were performed by using a fixed complex concentration to which increments of the DNA stock solutions were added. Copper(II) complex–DNA solutions were allowed to incubate for 10 min before the absorption spectra were recorded. Titration curves were constructed from the fractional change in the absorption intensity as a function of DNA concentration [25]. The intrinsic binding constant (K_b) can be obtained by the following equation:

$$[DNA]/(\varepsilon_a - \varepsilon_f) = [DNA]/(\varepsilon_b - \varepsilon_f) + 1/K_b(\varepsilon_b - \varepsilon_f) \quad (1)$$

where [DNA] is the DNA concentration in M (nucleotide), ε_a is the absorption coefficient observed at a given DNA concentration, ε_f is the absorption coefficient of a complex in the absence of DNA, ε_b is the absorption coefficient of a complex when fully bound to DNA, and K_b is the intrinsic binding constant in M^{-1}. Each set of data was fitted to the above equation, and the plot of [DNA]/($\varepsilon_a - \varepsilon_f$) *versus* [DNA] gave a slope and the *y*-intercept which is equal to $1/(\varepsilon_b - \varepsilon_f)$ and $1/K_b(\varepsilon_b - \varepsilon_f)$, respectively. The intrinsic binding constant K_b was obtained from the ratio of the slope to the intercept.

2.4.2. Fluorescence spectra. Fluorescence spectra were recorded with excitation at 480 nm and emission at 614 nm. The experiments were carried out by titrating complex (5 mM Tris–HCl/50 mM NaCl buffer) into the solution of DNA (1×10^{-4} M) and EtBr (8×10^{-5} M). Stern–Volmer quenching constant was calculated using the following expression [26]:

$$I_0/I = 1 + K_{sv}r \tag{2}$$

where I_0 and I are the fluorescence intensities in the absence and presence of complex, respectively, K_{sv} is the linear Stern–Volmer quenching constant dependent on the ratio of the bound concentration of EtBr to the concentration of DNA, and r is the total concentration of complex to that of DNA. In the plot of I_0/I *versus* [Complex]/[DNA], K_{sv} is given by the ratio of slope to the intercept.

2.4.3. Viscosity. Viscosity measurements were carried out using an Ostwald Viscometer maintained at a constant temperature of 28.0 ± 0.1 °C in a thermostatic bath. Flow time was measured with a digital stopwatch. Each sample was measured thrice and an average flow time was calculated. CT–DNA samples with approximately 200 base pairs in average length were prepared by soliciting in order to minimize the complexities arising from DNA flexibility. Data were presented as $(\eta/\eta_0)^{1/3}$ *versus* binding ratio [27], where η is the viscosity of DNA in the presence of complex and η_0 is the viscosity of DNA alone. The relative viscosity was calculated according to the relation $\eta = (t–t_0)/t_0$, where t_0 is the flow time for the buffer and t is the observed flow time for DNA in the presence and absence of the complex [28].

2.4.4. Cyclic voltammetric studies. Electrochemical techniques are complementary to other biophysical techniques that are applied to study the interaction between redox-active molecules and biomolecules. Double-distilled water was used to prepare the buffer solutions. CV was performed on a three-electrode system consisting of a GC electrode. Before each experiment, solutions were de-aerated by purging dry N_2 for 15 min and nitrogen was kept over the solution during the experiments [29].

2.5. *DNA cleavage*

The cleaving ability of a complex of supercoiled plasmid DNA (pBR322 DNA) was monitored using agarose gel electrophoresis. The DNA cleavage efficiency was monitored by targeting the basic components of plasmid DNA, and determining the ability of the complex to convert supercoiled DNA (Form I) to open circular (Form II) and linear forms (Form III). In the cleavage process, 1 μL of supercoiled DNA (33.3 μM) was treated with increasing

concentration of complex (10–60 μM) in Tris-HCl/NaCl buffer. A loading buffer containing 0.25% bromophenol blue, 0.25% xylene cyanol, and 30% glycerol (3 μL) was added, and the electrophoresis of the DNA cleavage products were performed on 0.8% agarose gel containing EtBr (1 μg/mL). After incubation for 30 min, the gels were run at 100 V for 1 h in TAE buffer (40 mM Tris base, 20 mM acetic acid, 1 mM EDTA, pH 7.4). The bands were viewed by placing the gel on an UV illuminator and were imaged.

3. Results and discussion

3.1. *Synthesis and general aspects*

A new copper(II) complex, $[Cu(epoxy)(phen)(NO_3)](NO_3)\cdot H_2O$, has been synthesized by reacting $Cu(NO_3)_2\cdot 3H_2O$ with 5,6-dihydro-5,6-epoxy-1,10-phenanthroline and 1,10-phenanthroline. The copper(II) complex is soluble in water and most organic solvents. The complex is paramagnetic with a single unpaired electron at room temperature, corresponding to d^9 electronic configuration for the copper(II) center. Elemental analysis data indicate that the metal to epoxy ligand and phen ligand ratio is 1 : 1 : 1, which is consistent with the obtained spectral results. The electronic absorption spectrum of the complex exhibits three intense intra-ligand charge transfer transitions attributed to π–π^* and n–π^*. Typically, spectra of octahedrally coordinated Cu(II) complexes exhibit a broad band frequently with shoulder(s) in the visible region, 1000–670 nm, assignable to a $^2E_g \rightarrow {}^2T_{2g}$ transition. Multiple states arise due to the splitting of the ^2D state of Cu(II) in a regular octahedral field. The electronic absorption spectra of the present Cu(II) complex show bands at *ca.* 14,184 cm^{-1} (705 nm, $\varepsilon = 67\ M^{-1}\ cm^{-1}$), assigned to a $^2E_g \rightarrow {}^2T_{2g}$ transition (figure S1) [30]. The IR spectrum of the complex shows a broad band at 3500 cm^{-1} attributed to the O–H stretch of water present in the lattice. The C–O stretch for epoxide was observed at 1583 cm^{-1} [31]. The bands at 1518 and 1427 cm^{-1} are attributed to the ring stretching frequencies of ν(C=C) and ν(C=N) in the phenanthroline ligands, respectively. The bands at 1346 and 1031 cm^{-1} are assigned to coordinated nitrate, whereas the band at 1383 cm^{-1} is attributed to uncoordinated nitrate [32, 33] (figure S2).

3.2. *X-ray crystal structure analysis*

The ORTEP diagram of $[Cu(epoxy)(phen)(NO_3)](NO_3)\cdot H_2O$ with the atom numbering scheme is shown in figure 1. Crystal refinement data are tabulated in table 1, and selected bond lengths and angles are given in table 2. The complex crystallized in the monoclinic *P21/n* space group with two independent molecules in the crystallographic asymmetric unit, and a goodness-of-fit for $F^2 = 1.024$. The copper has distorted octahedral geometry, coordinated to two nitrogens of 5,6-dihydro-5,6-epoxy-1,10-phenanthroline, two nitrogens of 1,10-phenanthroline, and two oxygens of the nitrate. Jahn–Teller distortion results in the Cu (1)–N(2) (2.074(5) Å) and Cu(1)–N(3) (2.066(5) Å) bonds being significantly longer than other bonds [34]. The two shortest bonds are Cu(1)–N(1) (1.955(5) Å) and Cu(1)–N(4) (1.958(6) Å). The bidentate nitrate ion coordinates via O2 and O3 forming a strained four-membered chelate ring (Cu1O2–N5O3) with a bite angle of 49.75° (O3–Cu1–O2). The copper-nitrogen bond lengths vary from 1.955 to 2.074 Å [35]. The Cu1–O3 bond length is longer (2.627 Å) than the Cu1–O2 bond length (2.315 Å). This is most likely due to the small bite angle (49.75°) of the bidentate nitrate ligand, which leads to distortion in the

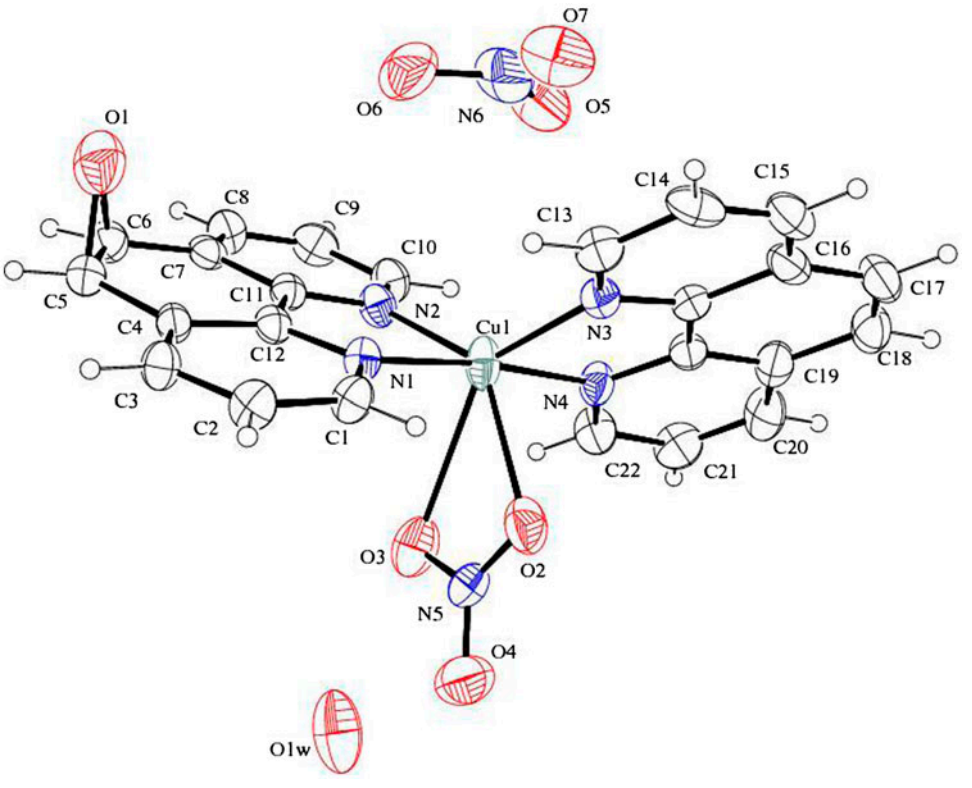

Figure 1. ORTEP diagram of $[Cu(epoxy)(phen)(NO_3)](NO_3)\cdot H_2O$. Displacement ellipsoids are drawn at the 40% probability level.

geometry of the complex [36]. Both the X-ray data and molar conductance (Λ_M) value of the complex in water (98 Ω^{-1} cm^2 mol^{-1}, 1×10^{-3} M) are consistent with the complex having a + 1 charge.

3.3. *Spectral studies of the interactions with DNA*

The B-form of CT–DNA is a polyanion composed of two complementary polymeric subunits hydrogen bonded together in the form of a right-handed double helix [37]. When the copper(II) complex interacts with DNA, it is likely to replace two sodium ions from the compact inner (Stern) layer or the diffuse outer layer surrounding DNA, and interact with the anionic phosphate residues of DNA [38]. Literature data demonstrate that the binding of metal complexes with DNA usually takes place through both covalent (via replacement of a labile group of the complex by a nitrogen donor from the nucleotide of DNA such as guanine N7) and/or non-covalent interactions (groove binding, intercalation, and electrostatic interactions) [39].

Electronic absorption spectroscopy is typically employed to evaluate the DNA binding mode and affinity of the metal complex for DNA. Since the d–d band of the complex is weak, a ligand-based electronic transition (π–π^*) was used to monitor the interaction of the complex with CT–DNA. The absorption intensity of complex increased (hyperchromism)

Table 1. Crystal data and structure refinement for $[Cu(epoxy)(phen)(NO_3)](NO_3)\cdot H_2O$.

Identification code	Shelxl
Empirical formula	$C_{24}H_{16}CuN_6O_8$
Formula weight	579.97
Temperature	293(2) (K)
Wavelength	0.71073 (Å)
Crystal system, space group	Monoclinic, *P21/n*
Unit cell dimensions	a = 13.3199(8) Å, α = 90°
	b = 11.2917(7) Å, β = 107.827(4)°
	c = 16.0832(9) Å, γ = 90°
Volume	2302.8(2) (Å^3)
Z, Calculated density	4, 1.673 (Mg m^{-3})
Absorption coefficient	1.015 (mm^{-1})
F(0 0 0)	1180
Crystal size	0.25 × 0.20 × 0.20 mm
Theta range for data collection	2.24–24.99°
Limiting indices	$-15 <= h <= 12$, $13 <= k <= 13$, $-18 <= l <= 19$
Reflections collected/unique	17,617/3949 [R(int) = 0.1607]
Completeness to θ = 24.99	97.4%
Absorption correction	Semi-empirical from equivalents
Max. and min. transmission	0.8228 and 0.7654
Refinement method	Full-matrix least-squares on F^2
Data/restraints/parameters	3949/119/405
Goodness-of-fit on F^2	1.024
Final R indices [$I > 2\sigma(I)$]	$R1$ = 0.0647, $wR2$ = 0.1872
R indices (all data)	$R1$ = 0.2454, $wR2$ = 0.2313
Largest diff. peak and hole	0.837 and −0.719 (e A^{-3})

Table 2. Selected bond lengths [Å] and angles [°] for $[Cu(epoxy)(phen)(NO_3)](NO_3)\cdot H_2O$.

N(1)–Cu(1)	1.955(5)
N(2)–Cu(1)	2.074(5)
N(3)–Cu(1)	2.066(5)
N(4)–Cu(1)	1.958(6)
O(2)–Cu(1)	2.316(5)
O(3)–Cu(1)	2.627(5)
N(1)–Cu(1)–N(4)	173.5(2)
N(1)–Cu(1)–N(3)	100.8(2)
N(4)–Cu(1)–N(3)	81.5(2)
N(1)–Cu(1)–N(2)	81.8(2)
N(4)–Cu(1)–N(2)	101.0(2)
N(3)–Cu(1)–N(2)	134.2(2)
N(1)–Cu(1)–O(2)	87.1(2)
N(4)–Cu(1)–O(2)	86.9(2)
N(3)–Cu(1)–O(2)	87.60(18)
N(2)–Cu(1)–O(2)	137.97(19)
O(2)–Cu(1)–O(3)	49.75(2)
N(5)–O(2)–Cu(1)	104.3(4)

and a blue shift was observed with the incremental addition of DNA (figure 2). These results support the complex intercalating with DNA, which involves a strong stacking interaction of the planar aromatic rings of the coordinated ligand with the base pairs of DNA [40].

A binding constant, K_b of $(4.8 \pm 0.2) \times 10^4$ M^{-1} was determined from the plot of [DNA]/($\varepsilon_a - \varepsilon_f$) *versus* [DNA] (inset of figure 2). The K_b value is higher than values reported for related Cu(II) complexes, including $[Cu(phen)_2Cl_2]$ (2.75×10^3 M^{-1}) [41], $[Cu_2(phen)_2Cl_4]$

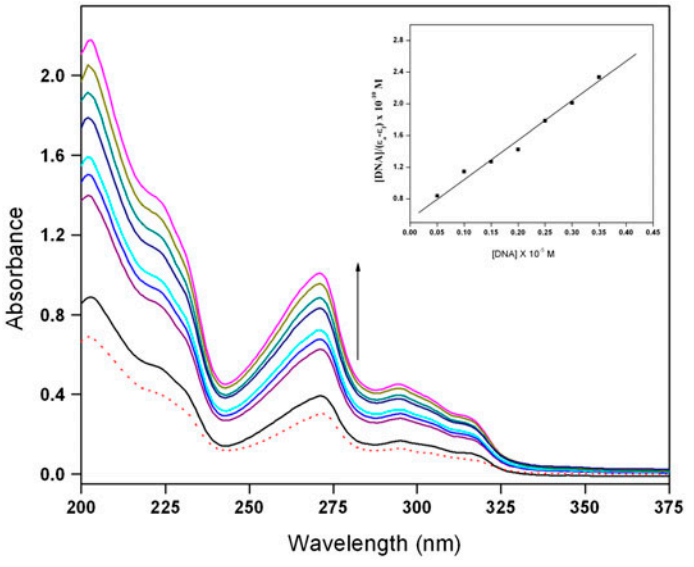

Figure 2. Absorption spectral traces on addition of CT DNA to $[Cu(epoxy)(phen)(NO_3)](NO_3)\cdot H_2O$ (shown by arrow). Inset plot of $[DNA]/(\varepsilon_a - \varepsilon_f)$ *vs*. [DNA] for absorption titration of CT DNA with complex. At 271 nm.

$(4.75 \times 10^4\ M^{-1})$ [42], $[Cu(phen)(L\text{-}Thr)H_2O]ClO_4$ $(6.35 \times 10^3\ M^{-1})$ [43], [Cu(Sal-L-val) phen] $(6.48 \times 10^3\ M^{-1})$ [44]. $[Cu(naph\text{-}Leu)(phen)]CH_3OH\cdot 5H_2O$ $(4.87 \times 10^3\ M^{-1})$ [45], $[Cu(phen)(pro)(H_2O)]ClO_4^-$ $(3.86 \times 10^3\ M^{-1})$ [46] and $[Cu(bipy)(pro)(H_2O)]ClO_4^-$ $(4.6 \times 10^3\ M^{-1})$ [25].

3.4. *Fluorescence studies*

Fluorescence spectroscopy is another useful method to probe the binding of the complexes to CT–DNA. The emission intensity of ethidium bromide was used as a spectral probe. The intrinsic fluorescence intensities of DNA and ethidium bromide in Tris–HCl buffer are low, whereas the fluorescence intensity of ethidium bromide is enhanced upon addition of DNA due to intercalation. If the complex also intercalates strongly with DNA, the ethidium bromide binding to DNA will decrease, resulting in an observed decrease in fluorescence [47]. In our experiments, the fluorescence intensity attributed to ethidium bromide binding to DNA at 614 nm decreased significantly with increasing concentration of the complex (figure 3). This may be either due to the metal complex competing with ethidium bromide for the DNA binding sites, thus displacing the ethidium bromide (whose fluorescence is enhanced upon DNA binding), or alternatively a direct quenching interaction with DNA itself. It is likely that the former occurs, as observed for other copper(II) complexes [48, 49]. The binding constant, K_b, is $(2.5 \pm 0.2) \times 10^4\ M^{-1}$.

3.5. *Viscosity measurements*

To further explore the binding mode of the copper(II) complex with DNA, viscosity measurements were carried out. Since the relative specific viscosity (η/η_0) (η and η_0 are the

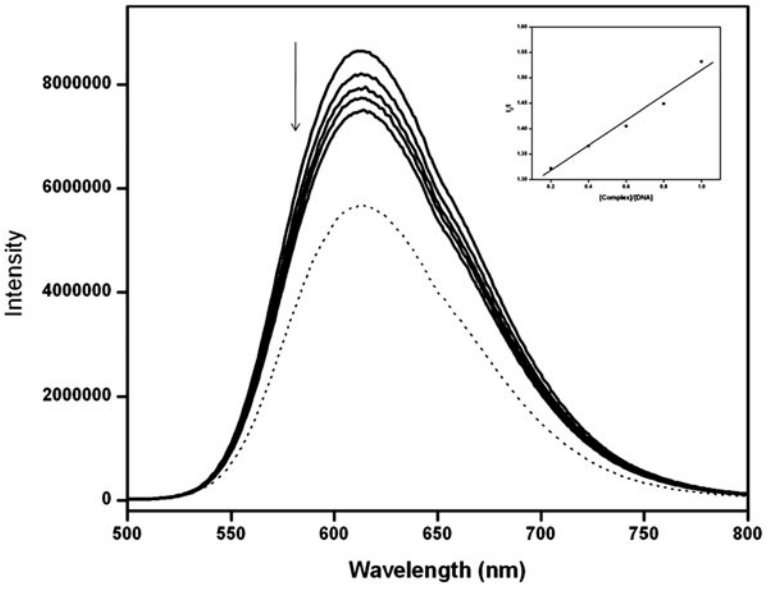

Figure 3. Fluorescence emission spectra (excited at 480 nm) of the CT DNA-EB system (4×10^{-5} M ethidium bromide, 4×10^{-5} M CT DNA) in the absence (dotted line) and presence (dashed line) of $0.8–4.0 \times 10^{-5}$ M $[Cu(epoxy)(phen)(NO_3)](NO_3)\cdot H_2O$.

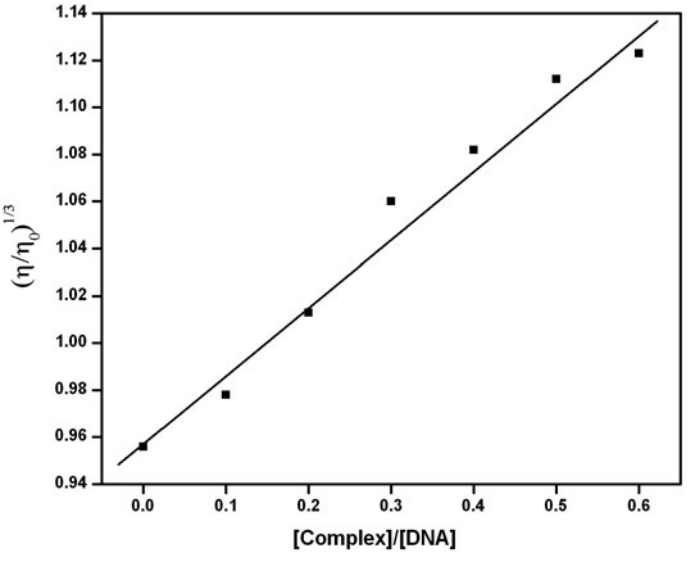

Figure 4. Effect of increasing amounts of complex on the relative viscosity of calf thymus DNA at 27 °C.

specific viscosities of DNA in the presence and absence of the complex, respectively) of DNA reflects the increase in contour length associated with the separation of DNA base pairs caused by intercalation, a classical intercalator, such as ethidium bromide could cause

a significant increase in viscosity of DNA solutions. In contrast, a partial and/or non-classical intercalation of the ligand could bend or kink the DNA, resulting in a decrease in its effective length with a concomitant increase in its viscosity [50, 51], while the electrostatic and groove binding cause little or no effect on the relative viscosity of DNA solutions [52]. Therefore, viscosity measurements, which are sensitive to the changes in the contour length of DNA, are useful to probe for DNA intercalation by complexes.

The plots of relative specific viscosities *versus* $1/R = ([\text{Complex}]/[\text{DNA}])$ are shown in figure 4. The relative specific viscosity increases with increasing concentration of the complex. However, the increase in the viscosity was much less compared to that of classical intercalators like ethidium bromide in the same DNA concentration range [53]. This observation supports the above spectral studies which suggest that the complex weakly intercalates with the DNA base pairs. Partial intercalation results in lengthening of the DNA helix due to base pairs being separated to accommodate the binding ligand, leading to an increase in the viscosity of the solution.

3.6. *Cyclic voltammetric studies*

The application of CV to study the interaction between complex and DNA provides a useful complement to UV–vis and fluorescence spectroscopy and viscosity experiments. A cyclic voltammogram of a 0.01 mM complex solution in the absence and presence of DNA using a GC electrode in DMF was recorded (figure S3). In the forward scan, a single cathodic peak was observed at −0.84 V, which corresponds to the reduction of the copper(II) center (Cu^{II}–Cu^{I}). In the reverse scan, an anodic peak is not observed, which indicates that the process is irreversible. When CT–DNA is added to this complex solution, the cathodic peak was observed at −0.78 V, and no new reduction waves appeared. The observed decrease in current intensity is attributed to the diffusion of an equilibrium mixture of free and DNA-bound complex to the electrode surface. Thus, the slower mass transfer of complexes bound to DNA fragments leads to a decrease in concentration of the unbound redox-active species in solution [54]. The positive shift of the reduction potential supports the complex intercalating with CT–DNA.

3.7. *Nuclease activity*

DNA cleavage is also a useful method to probe DNA–complex interactions [55]. In DNA cleavage experiments, the supercoiled circular form of pBR322 DNA is converted into nicked and linear circular forms of DNA. When the resultant DNA is analyzed by gel

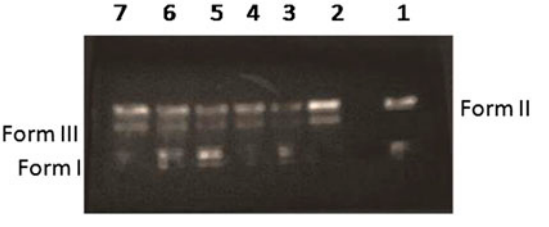

Figure 5. Electrophoretic behavior of pBR322 DNA by $[Cu(epoxy)(phen)(NO_3)](NO_3)\cdot H_2O$. Lane 1, DNA alone; lanes 2–7: DNA + copper(II) complex in the concentration of 10, 20, 30, 40, 50, 60 μM, respectively.

electrophoresis, the fastest migration will be observed for the supercoiled form (Form I). If one strand is cleaved, the supercoiled form relaxes to produce a slower moving open circular form (Form II). If both strands are cleaved, a linear form (Form III) will be generated that migrates slower than Form I and faster than Form II. Interestingly, we have found that this mixed-ligand copper(II) complex can cleave the supercoiled DNA to give circular and linear DNA. As shown in figure 5, with increasing complex concentration, the amount of Form I DNA decreases, while that of Form II and Form III DNA increases. When the complex concentration was as high as 10 μM (lane 2), Form II was observed, whereas with 20 μM or above (lanes 4–7), the supercoiled DNA (Form I) band disappeared completely, and only Forms II and III were observed. The presence of aromatic moiety and hard Lewis acid properties of complexes could play a vital role in the DNA cleavage process by a hydrolytic pathway.

3.8. *Luminescence properties*

The photoluminescence of the copper(II) complex was studied at room temperature in DMSO solution. The emission spectrum of the copper(II) complex exhibits a blue-green band at 408–448 nm upon excitation at 362 nm (figure S4). This band is assigned to an intra-ligand π–π^* transition [56].

4. Conclusion

A new copper(II) complex, $[Cu(epoxy)(phen)(NO_3)](NO_3)\cdot H_2O$ (epoxy = 5,6-dihydro-5,6-epoxy-1,10-phenanthroline; phen = 1,10-phenanthroline), has been synthesized and characterized using elemental analysis, IR and UV–vis spectroscopy, and single crystal X-ray crystallography. In agreement with the electronic spectrum, X-ray diffraction data show a distorted octahedral geometry for the Cu(II) complex with a CuN_4O_2 coordination sphere. The interaction of the complex with DNA was investigated by UV and fluorescence spectroscopy, viscosity measurements, CV, and gel electrophoresis. A weak intercalative binding mode of the complex with DNA is proposed based on the data, and the complex cleaves plasmid DNA efficiently. These results suggest considerable potential for mixed-ligand complexes of this type as chemotherapeutic agents.

Supplementary material

CCDC 973086 contains the supplementary crystallographic data of epoxy copper(II) complex. These data can be obtained free of charge from the Cambridge Crystallographic Data Center (CCDC), 12 Union Road, Cambridge CB2 1EZ, UK; Fax: (+44) 1223–336-033; or E-mail: deposit@ccdc.cam.ac.uk.

Acknowledgments

We are grateful to IIT-M, Chennai for providing instrumental facilities, including IR spectroscopy, X-ray crystallography, and fluorescence spectroscopy.

Disclosure statement

No potential conflict of interest was reported by the authors.

Supplemental data

The supplemental data for this article is available online at http://dx.doi.org/10.1080/00958972.2015.1088526.

References

[1] X. Zhang, C. Bi, Y. Fan, Q. Cui, D. Chen, Y. Xiao, Q.P. Dou. *Int. J. Mol. Med.*, **22**, 677 (2008).
[2] S. Tabassum, W.M. Al-Asbahy, M. Afzal, F. Arjmand. *J. Photochem. Photobiol., B*, **114**, 132 (2012).
[3] A. Spassky, D.S. Sigman. *Biochemistry*, **24**, 8050 (1985).
[4] D.K. Chand, H.J. Schneider, A. Bencini, A. Bianchi, C. Giorgi, S. Ciattini, B. Valtancoli. *Chemistry*, **6**, 4001 (2000).
[5] J. Lakshmipraba, S. Arunachalam, R. Vijay Solomon. *J. Coord. Chem.*, **68**, 1374 (2015).
[6] G. Chelucci, R.P. Thummel. *Chem. Rev.*, **102**, 3129 (2002).
[7] E. Schoffers. *Eur. J. Org. Chem.*, **2003**, 1145 (2003).
[8] C.R. Luman, F.N. Castellano, In *Phenanthroline Ligands*, J.A.M. McCleverty, J. Thomas (Eds), Vol. 1, p. 25–39, *Compr. Coord. Chem., II*; Elsevier, Oxford (2004).
[9] A. Bencini, V. Lippolis. *Coord. Chem. Rev.*, **254**, 2096 (2010).
[10] P.G. Sammes, G. Yahioglu. *Chem. Soc. Rev.*, **23**, 327 (1994).
[11] B. Chesneau, A. Passelande, P. Hudhomme. *Org. Lett.*, **11**, 649 (2009).
[12] G. Accorsi, A. Listorti, K. Yoosaf, N. Armaroli. *Chem. Soc. Rev.*, **38**, 1690 (2009).
[13] S. Krishnan, D.J. Kuhn, G.A. Hamilton. *J. Am. Chem. Soc.*, **99**, 8121 (1977).
[14] N.K. Shee, D. Das, F.A.O. Adekunle, M.G.B. Drew, D. Datta. *Inorg. Chim. Acta*, **366**, 198 (2011).
[15] J.L. Jiang, R. Hua. *Synth. Commun.*, **36**, 3141 (2006).
[16] J.T. Tracy, T.D.P. Stack. *J. Am. Chem. Soc.*, **130**, 4945 (2008).
[17] H. Gopinathan, N. Komathi, M.N. Arumugham. *Inorg. Chim. Acta*, **93**, 416 (2014).
[18] P. Santhakumar, M.N. Arumugham. *Int. J. Recent Sci. Res.*, **3**, 459 (2012).
[19] Bruker. APEX2 and SAINT-Plus (version 7.06a), Bruker AXS Inc., Madison, WI (2004).
[20] Bruker. *SADABS*, Bruker AXS Inc., Madison, WI (1999).
[21] A. Altomare, G. Cascarano, C. Giacovazzo, A. Guagliardi. *J. Appl. Crystallogr.*, **26**, 343 (1993).
[22] G.M.Sheldrick. *Acta Crystallogr., Sect. A: Found. Crystallogr.*, **64**, 112 (2008).
[23] J. Marmur. *J. Mol. Biol.*, **3**, 208 (1961).
[24] M.E. Reichmann, S.A. Rice, C.A. Thomas, P. Doty. *J. Am. Chem. Soc.*, **76**, 3047 (1954).
[25] A. Wolfe, G.H. Shimer, T. Meehan. *Biochemistry*, **26**, 6392 (1897).
[26] M.T. Carter, M. Rodriguez, A.J. Bard. *J. Am. Chem. Soc.*, **111**, 8901 (1989).
[27] G. Cohen, H. Eisenberg. *Biopolymers*, **8**, 45 (1969).
[28] S. Satyanarayana, J.C. Dabrowiak, J.B. Chaires. *Biochemistry*, **32**, 2573 (1993).
[29] P. Gurumoorthy, D. Mahendiran, D. Prabhu, C. Arulvasu, A.K. Rahiman. *RSC Adv.*, **4**, 42855 (2014).
[30] N. Raman, A. Sakthivel, R. Jeyamurugan. *J. Coord. Chem.*, **63**, 4380 (2010).
[31] R.M. Silverstein, F.X. Webster, D.J. Kiemle. *Spectroscopic Identification of Organic Compounds*, 7th Edn., p. 91, John Wiley & Sons Inc. (2005).
[32] M. Vicente, C. Lodeiro, H. Adams, R. Bastida, A.D. Blas, D.E. Fenton, A. Macías, A. Rodríguez, T.R. Rodríguez-Blas. *Eur. J. Inorg. Chem.*, **2000**, 1015 (2000).
[33] C. Karthick, P. Gurumoorthy, M.A. Imran Musthafa, R. Lakra, P.S. Korrapati, A.K. Rahiman. *J. Coord. Chem.*, **67**, 1794 (2014).
[34] J.P. Naskar, S. Hati, D. Datta, *Acta Crystallogr., Sect. B: Struct. Sci.*, **53**, 885 (1997).
[35] I. Banerjee, J. Marek, R. Herchel, M. Ali. *Polyhedron*, **29**, 1201 (2010).
[36] P.L. Maheswari, B. Modec, A. Pevec, B. Kozlevčar, C. Massera, P. Gamez. *Inorg. Chem.*, **45**, 6637 (2006).
[37] W. Saenger. *Principles of Nucleic Acid Structure*, Vol. 253, Springer, New York (1983).
[38] G.S. Manning. *Q. Rev. Biophys.*, **11**, 179 (1978).
[39] N. Grover, T.W. Welch, T.A. Fairley, M. Cory, H.H. Thorp. *Inorg. Chem.*, **33**, 3544 (1994).
[40] V.A. Bloomfield, D.M. Crothers, I. Tinocco Jr. *Physical Chemistry of Nucleis Acids*, Vol. 432, Harper & Row, New York (1974).
[41] T. Gupta, S. Dhar, M. Nethaji, A.K. Chakravarty. *Dalton Trans.*, 1896 (2004).

[42] Q.Q. Zhang, F. Zhang, W.G. Wang, X.L. Wang. *J. Inorg. Biochem.*, **100**, 13344 (2006).
[43] S. Zhang, Y. Zhu, C. Tu, H. Wei, Z. Yang, L. Lin, J. Ding, J. Zhang, Z. Guo. *J. Inorg. Biochem.*, **98**, 2099 (2004).
[44] J.F. Dong, L.Z. Li, G.H. Liu, T. Xu, D.Q. Wang. *J. Mol. Struct.*, **986**, 57 (2011).
[45] J.F. Dong, L.Z. Li, L.W. Li, T. Xu, D.Q. Wang. *Chin. J. Chem.*, **29**, 259 (2011).
[46] C.V. Kumar, E.H. Asuncion. *J. Am. Chem. Soc.*, **115**, 8547 (1993).
[47] R. Indumathy, S. Radhika, M. Kanthimathi, T. Weyhermuller, B.U. Nair. *J. Inorg. Biochem.*, **101**, 434 (2007).
[48] Z.Q. Liu, Y.T. Li, Z.Y. Wu, Y.L. Song. *Inorg. Chim. Acta*, **361**, 226 (2008).
[49] U. McDonnell, M.R. Hicks, M.J. Hannon, A. Rodger. *J. Inorg. Biochem.*, **102**, 2052 (2008).
[50] S. Satyanarayana, J.C. Dabrowiak, J.B. Chaires. *Biochemistry*, **31**, 9319 (1992).
[51] E.J. Gabbay, R.E. Scofield, C.S. Baxter. *J. Am. Chem. Soc.*, **95**, 7850 (1973).
[52] I. Haq, P. Lincoln, D. Suh, B. Norden, B.Z. Chowdhry, J.B. Chaires. *J. Am. Chem. Soc.*, **117**, 4788 (1995).
[53] B.-D. Wang, Z.-Y. Yang, P. Crewdson, D.-Q. Wang. *J. Inorg. Biochem.*, **107**, 1492 (2007).
[54] M.C. Prabahkara, H.S.B. Naik. *BioMetals*, **21**, 675 (2008).
[55] A.S. Sitlani, E.C. Long, A.M. Pyle, J.K. Barton. *J. Am. Chem. Soc.*, **114**, 2303 (1992).
[56] N.J. Turro. *Pure Appl. Chem.*, **49**, 405 (1977).